

MEMO

PROJECT	Concept development, floating bridge E39 Bjørnafjorden	DOCUMENT CODE	10205546-11-NOT-210
CLIENT	Statens vegvesen	ACCESSIBILITY	Restricted
SUBJECT	Preliminary evaluation of viscous damper between tower and bridge girder	PROJECT MANAGER	Svein Erik Jakobsen
TO	Statens vegvesen	PREPARED BY	Mads Fredrik Heiervang / Per Norum Larsen / Knut Andreas Kvåle
COPY TO		RESPONSIBLE UNIT	AMC

CONTENT

This note describes the preliminary evaluation of the viscous damper between tower and bridge girder. By releasing the lateral constraint of the bridge girder at the tower and in the back spans, the bridge girder can vibrate at the tower position. This allows for dashpots to be positioned at the connection to the tower, to introduce linear damping in the system. Thus, the critical damping of the longest transverse eigenmodes can be increased in order to ensure that (i) parametric resonance is avoided and (ii) the resonant swell response is limited.

A numerical analysis of the proposed design measure has been simulated in Orcaflex, and the response has been compared to the response of the basecase K12 model. The results show that the strong axis moment swell response may be reduced by approx. 60%, and the axial force swell response may be reduced by approx. 30%.

An evaluation of parametric resonance has been performed for the K11 concept by modal analysis and estimating the critical axial force, accounting for the increased damping from the dashpot system. The results show that the dashpot system is an efficient measure for increasing the critical axial force, thus increasing the robustness towards parametric resonance. By this measure, the onset criterion for parametric resonance may be satisfied.

The analyses presented in this note is based on lateral constraints on the back span columns, which may prove difficult to design. However, the columns supported back span may be replaced by a free span back span, thus removing the need of gliding bearings. The effect of a free span back span, which may reduce the length between the abutment and the tower, has not been considered.

0	20.02.2020	Preliminary evaluation of viscous damper between tower and bridge girder	MFH/PNL/KAK	Per Norum Larsen	Per Norum Larsen
REV.	DATE	DESCRIPTION	PREPARED BY	CHECKED BY	APPROVED BY

TABLE OF CONTENTS

1	Overview	3
2	Global analysis (K12).....	4
2.1	Model description.....	4
2.2	Environmental conditions.....	4
2.3	Results from global analysis	5
3	Parametric resonance (K11)	7

1 Overview

The end-anchored floating bridge concepts for Bjørnafjorden have long eigenmodes with low damping, which results in relatively high response and the bridge may be vulnerable for parametric resonance. This memo contains a preliminary evaluation of a proposed design measure for the floating bridge crossings of Bjørnafjorden. By releasing the lateral constraint of the deck at the tower and in the back spans, the bridge girder can vibrate at the tower position. This allows for dashpots to be positioned at the connection to the tower, to introduce linear damping in the system. Thus, the critical damping of the longest transverse eigenmodes can be increased in order to ensure that (i) parametric resonance is avoided and (ii) the resonant swell response is limited.

In the analysis and evaluation of parametric resonance, a single dashpot system has been modelled between the tower and the deck. However, in design it is proposed to use four linear viscous dampers as illustrated in Figure 1-1. The oscillating periods of the dashpots is listed in Table 2-3. If this option is considered further, we recommend contacting manufacturers for evaluation of constructability.

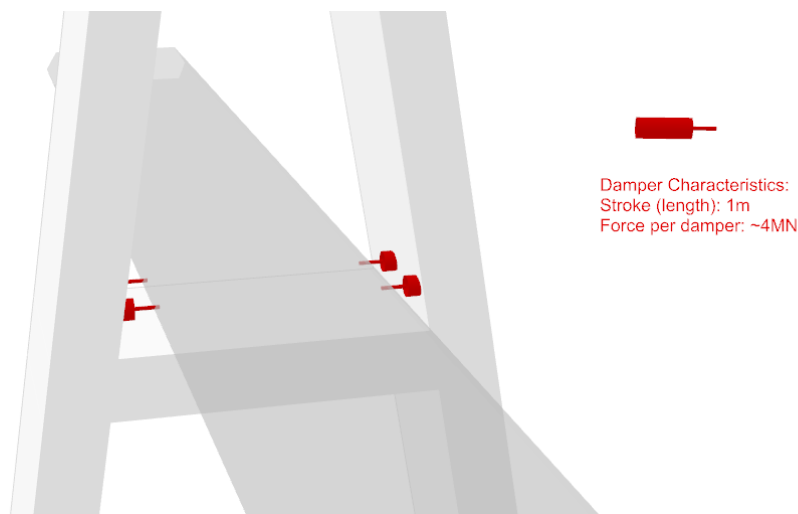


Figure 1-1 Indicative illustration and numbers for the four dashpots between tower and deck. Estimation of force per damper is based on the given stroke length estimated from Table 2-3, and a resulting oscillating period of 13s.

In the analyses the deck is free to translate laterally on the back span columns. These gliding bearings may prove difficult to design, but the columns may be replaced by a shorter free-span back span. The shorter back span may decrease the length between the abutment and the dashpots (at the tower), resulting in a lower dampening level of the long eigenmodes. However, the effect has not been quantified.

2 Global analysis (K12)

2.1 Model description

A numerical model has been established in Orcaflex, adapted from the K12 basecase model presented in Appendix F. For simplification, the girder is modelled as free to translate laterally in the back span and supported in the back span vertically, for illustration see Figure 2-1. In a further evaluation of the alternative, a back span without columns should be modelled. The rigid lateral connection between the tower cross beam and girder is replaced by a linear damper with 30MN/m.

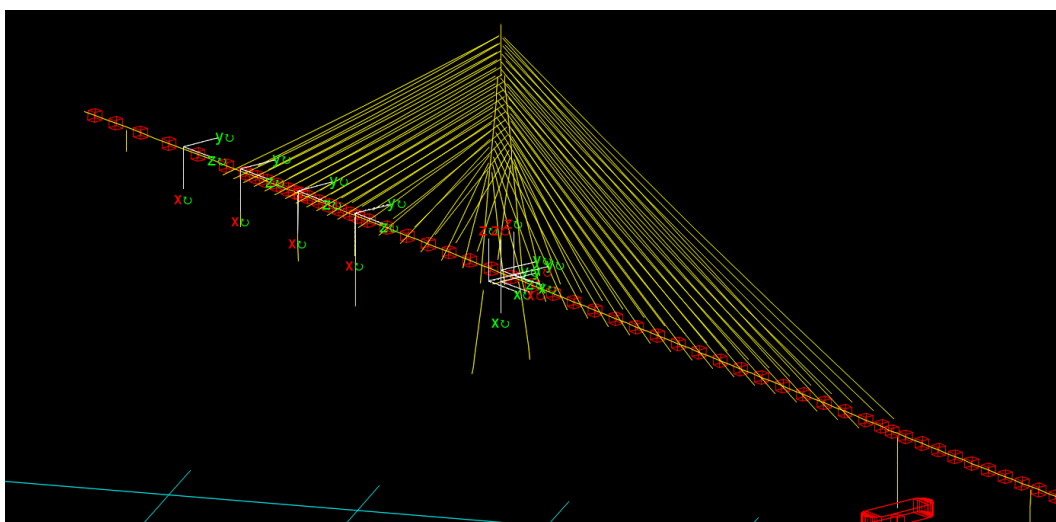


Figure 2-1: Snapshot of the cable-stayed tower part of the numerical model in Orcaflex

2.2 Environmental conditions

For comparison of the K12 basecase and the tower damper alternative the 100 year wind, windsea and swell conditions have been simulated in Orcaflex. The selected sea states are presented in Table 2-1 and Table 2-2.

Table 2-1: Selected design load cases for the 100year wind waves

	Design case 1	Design case 2	Design case 3	Design case 4
Hs [m]	2.1	1.4	2.0	2.0
Tp [s]	5.5	4.6	5.2	5.2
Wave Direction [deg]	105	195	295	315

Table 2-2: Selected design load case for the 100year swell. Note that the swell conditions have been applied at the critical eigenmode for both the K12 basecase and the tower damper alternative.

	Design case 1	Design case 2

Hs [m]	0.34	0.34
Tp [s]	17.0 /18.1	13.5 / 13.0
Wave Direction [deg]	300	305

2.3 Results from global analysis

Selected results from the Orcaflex analysis are compared in Figure 2-3. At the tower there is a significant reduction of the strong axis bending moment for all considered load cases, including static cases. However, the redistribution of forces results in a significant increase of bending moment towards the end abutment in south.

The maximum strong axis bending moment in the bridge girder is significantly reduced for the swell design case, see a comparison of envelope values in Figure 2-3. A comparison of the resulting von-Mises stress in ULS3 is presented in Figure 2-2. For the tower damper alternative the maximum stress in the main span is reduced with roughly 30% when compared to the K12 basecase.

For the K12 tower damper alternative the horizontal translation at the location of the damper has been extracted, see Table 2-3. The dominating oscillating period is given in the parenthesis. From the results it is estimated that the necessary length of stroke for the damper is a minimum of 1m in each direction.

The axial force response in the bridge girder from swell is an important parameter for evaluation of parametric resonance. The axial force response of the tower damper alternative is reduced with roughly 30% as compared to the K12 basecase.

Table 2-3: Selected results from analysis for comparison of basecase K12 concept (Basecase) with alternative K12 design with tower damper (TD). SA denotes strong axis, na denotes not available results.

	SA bending moment at tower [kNm]		Maximum SA bending moment [kNm]		Translation in tower [mm]	
	Basecase	TD	Basecase	TD	Basecase	TD
Windsea 100 year	490	350	800	800	0	100 (6s)
Swell 100 year	850	250	1100	400	0	170 (18s)
Dynamic wind 100year	720	460	790	750	0	400 (~35s)
Combined dynamic	na	na	na	na	0	560
Static wind 100 year	na	na	na	na	0	420

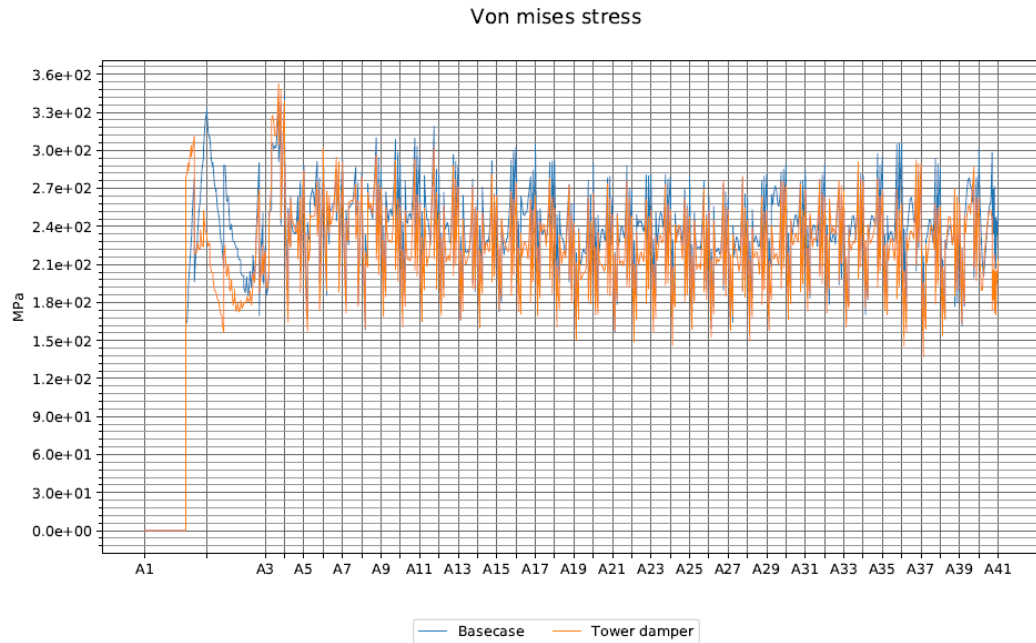


Figure 2-2: Comparison of maximum ULS3 von-Mises stress in bridge girder between K12 basecase concept and K12 alternative with tower damper. The maximum stress of the four corner points in the cross section from every design sea state is calculated and compared.

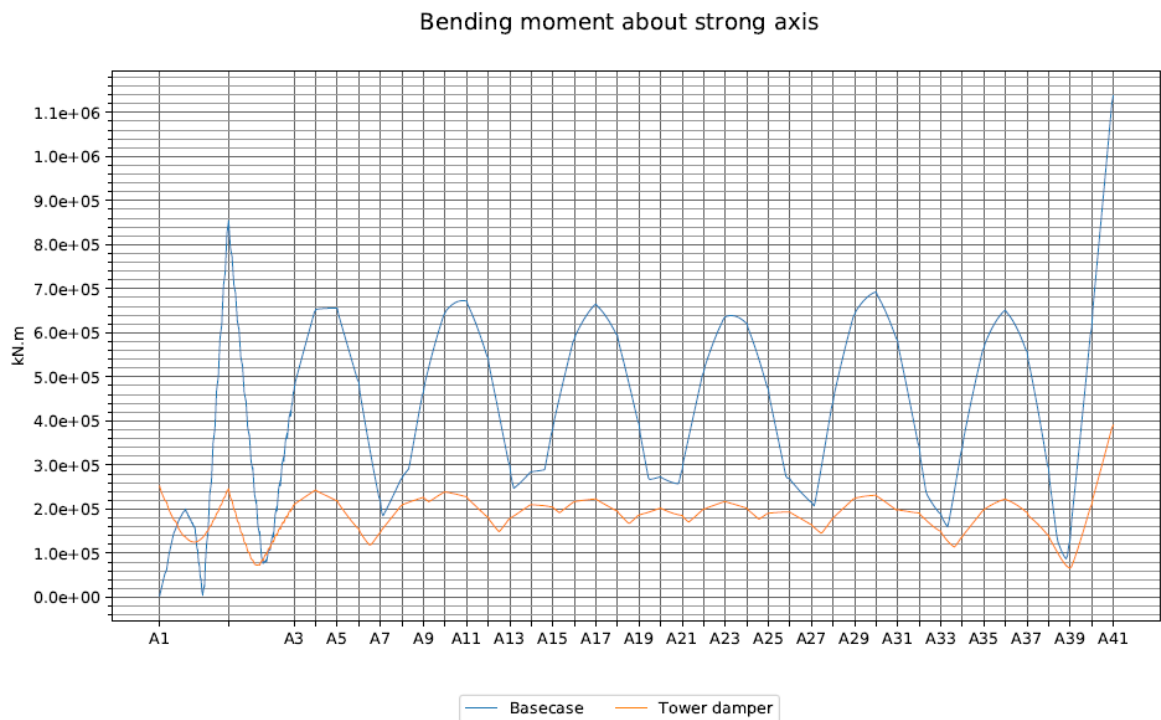


Figure 2-3: Comparison of maximum bending moment about strong axis from swell between K12 basecase concept and K12 alternative with tower damper.

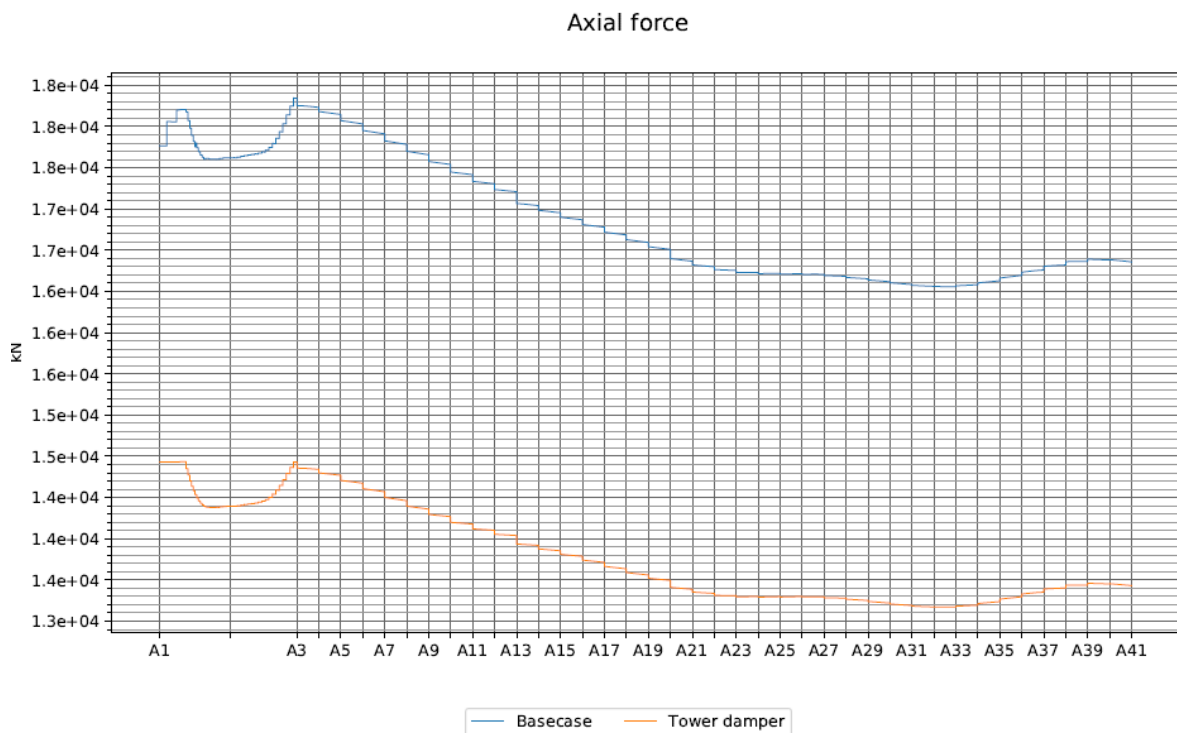


Figure 2-4: Comparison of axial force from swell between K12 basecase concept and K12 alternative with tower damper.

3 Parametric resonance (K11)

(extracted from section 9 in appendix S)

Modal analysis has been conducted in the same manner as described in Appendix S section 3.6, and more in-depth, in Appendix F, Section 6.2. By not introducing any assumptions about the damping in the modal analysis, in contrast to traditional modal analysis where the damping is assumed classical, the physics of the introduction of a damper is better represented. The following results are based on including hydrodynamic contributions but disregarding aerodynamic contributions.

Figure 3-1 shows the critical damping ratio for modes 1–6 with varying damping constants on the discrete damper. As is observed from the figure, a damping constant maximizing the critical damping coefficient can be found for each mode. This fact is supported by the fact that when the damper is larger, the resulting mode shapes change such that the damper is less mobilized. A value of C in the range between $15 \text{ MN}/(m/s)$ and $20 \text{ MN}/(m/s)$ seems to provide a rather good damping contribution to all modes considered.

The critical damping ratio and corresponding critical axial force of modes 1–10 due to the introduction of a damper with characterized by $C = 15 \text{ MN}/(m/s)$ are compared with K11_07 in Figure 3-2. The comparison is made based on a linearized quadratic drag damping corresponding to a 1m displacement of the modes (one at the time). Some of the change in critical amplitude can be explained by the fact that the ratio k/\hat{k}_g is also changed (mode 6), as seen in Figure 3-3, but the largest effect is due to the drastically increased critical damping ratio.

By introducing a large non-classical damping contribution, an assessment of the degree of coupledness of the modes should be conducted before carrying out other analyses based on the diagonalized system. The effect of the damper with $C = 15 \text{ MN}/(m/s)$ on the modal phase

collinearity (MPC) factor, which is described in Appendix F, Section 6.2, is illustrated by comparing Figure 3-4 and Figure 3-5. As expected, the modes have larger phase differences between response values, which indicates a coupled response. This is something that must be investigated more in depth before drawing final conclusions about the increased robustness towards parametric resonance. However, the preliminary findings indicate a vastly improved robustness towards parametric resonance by introducing a damper. Other effects due to the introduction of a damper is not evaluated in this section.

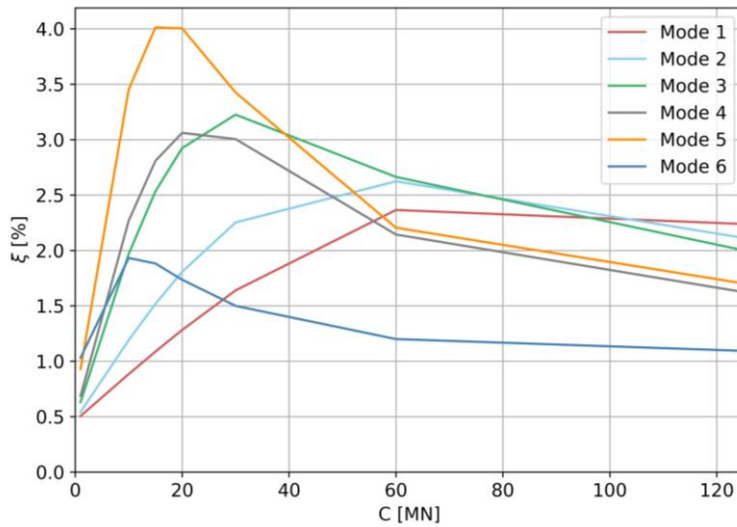


Figure 3-1. Optimal damper constant for the maximization of each modal critical damping ratio.

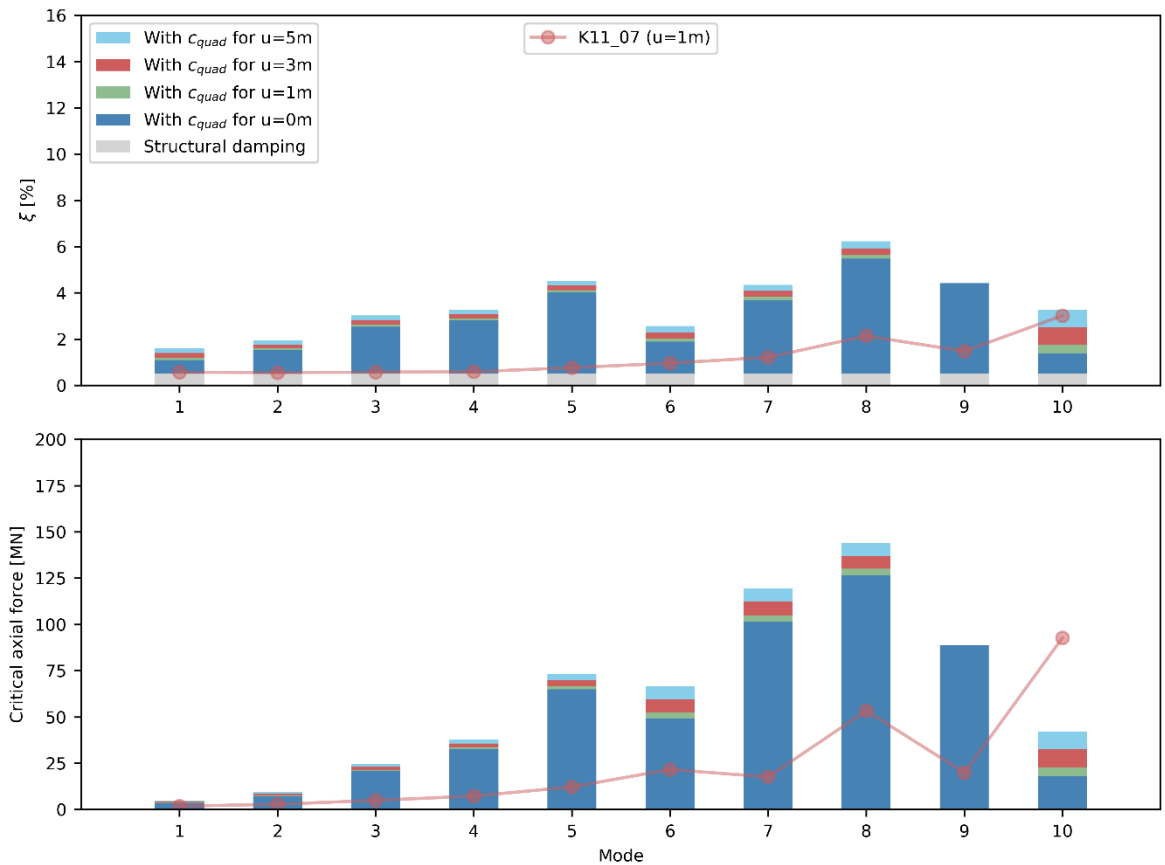


Figure 3-2. Comparison of K11_07 and the modified K12_07 (released lateral motion in tower and back span) with a discrete linear damper with $C = 15MN/(m/s)$.

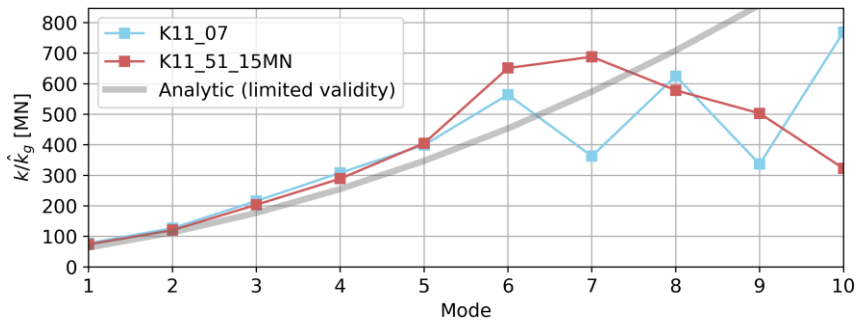


Figure 3-3. Ratio of total static stiffness to geometric stiffness per axial force.

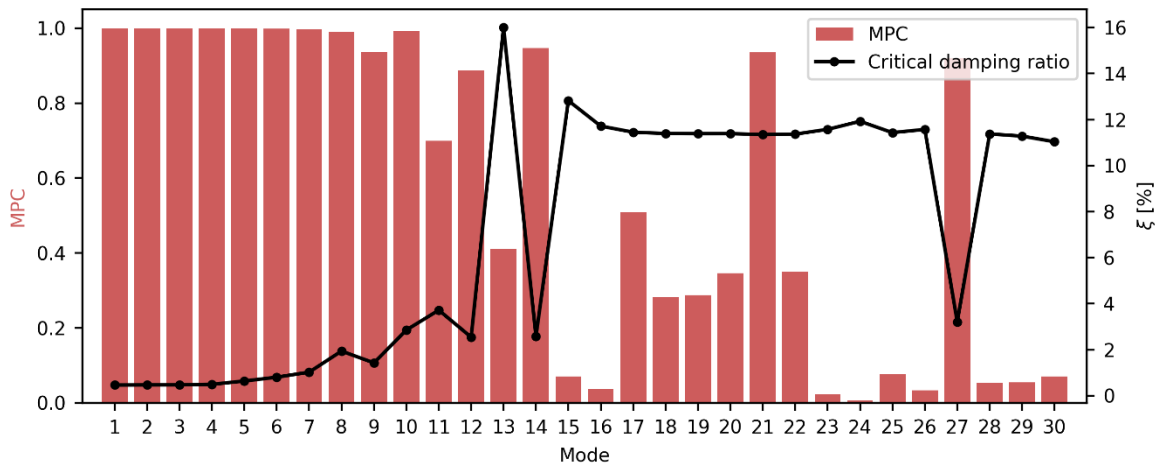


Figure 3-4. Modal phase collinearity (MPC) and critical damping ratio for 30 first modes of K12.

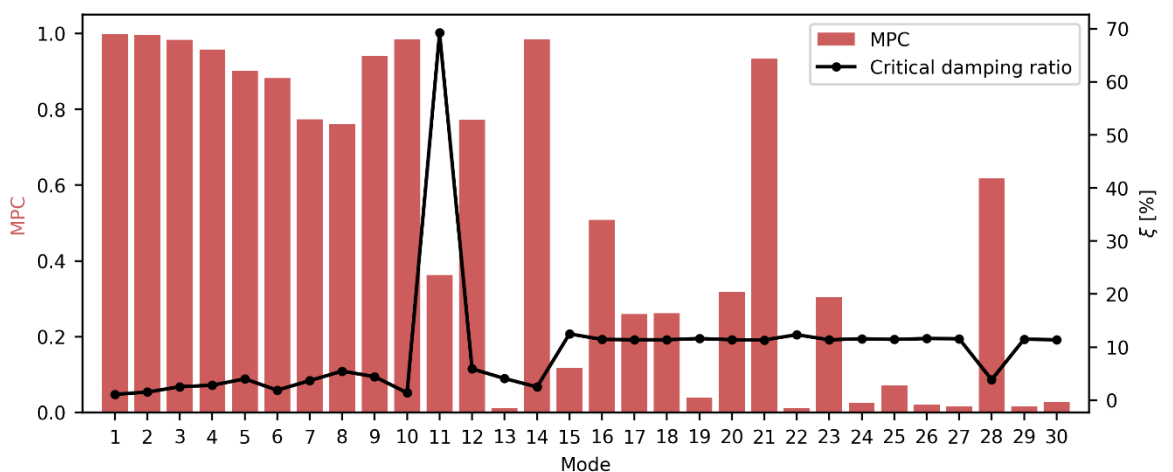


Figure 3-5. Modal phase collinearity (MPC) and critical damping ratio for 30 first modes of adjusted K12 model (released at tower and back span) with a discrete linear damper with $C = 15 \text{ MN}/(\text{m}/\text{s})$. The MPC is reduced when including the discrete damper.